Implementation of filter-clamped topology for transformerless three-phase PV inverters with reduced leakage current

Mohammed Abdullah[1,2], S. Venkata Padmavathi[1]
[1]Department of Electrical, Electronics and Communication Engineering, GSCE, GITAM (Deemed to be University), Hyderabad, India
[2]Department of Electrical and Electronics Engineering, Muffakham Jah College of Engineering and Technology, Hyderabad, India

Article Info

Article history:

Received Nov 25, 2025
Revised Jun 4, 2026
Accepted Jul 8, 2026

Keywords:

Filter-clamped inverter
Full-bridge inverter
Grid-connected inverter
Leakage current reduction
TLPV inverter

ABSTRACT

The growing prevalence of grid-connected photovoltaic (PV) systems has intensified the demand for efficient, reliable, and compact power conversion technologies. Transformerless photovoltaic (TLPV) systems provide improved efficiency and reduced size and costs compared to those using line-frequency or high-frequency isolation transformers. However, these inverters commonly exhibit leakage current because they lack galvanic isolation. Conventional topologies address this issue by adding extra semiconductor devices or employing complex control methods. This paper examines how a filter-clamped inverter (FCI) operates in grid-connected three-phase transformerless photovoltaic (TLPV) applications. However, the proposed inverter successfully reduces leakage current without additional components or control modifications. This makes it a compact and simplified alternative for transformerless PV applications. Additionally, the traditional full-bridge (FB) inverter with three phases, when compared to the FC inverter, has very high leakage current. Simulation results validate the FC inverter's ability to minimize leakage current.

Corresponding Author:

S. Venkata Padmavathi
Department of Electrical, Electronics, and Communication Engineering, GSCE
GITAM (Deemed to be University)
Hyderabad, Telangana, India
Email: vsatyava@gitam.edu

1. INTRODUCTION

Direct current (DC) produced by photovoltaic (PV) modules is processed by switched-mode power converters, enabling quicker control responses than those of other renewable energy sources. Both the expansion of distributed solar energy within communities and large investments in megawatt-scale central PV plants have been spurred by these benefits [1], [2]. Different from other renewable energy systems, PV inverters have unique features.

Three-phase inverters can employ smaller capacitive filters while maintaining constant voltage because, in the DC connection, they do not encounter double-line-frequency ripples, unlike single-phase systems [3]–[6]. This improves system reliability. The cost of solar energy is strongly impacted by the efficiency, dependability, and cost-effectiveness of the numerous inverters that make up large-scale PV systems. Because of their greater efficiency, three-phase PV inverters are more appropriate for high-power applications, despite the fact that residential distributed generation often uses single-phase inverters [7], [8].

Transformerless photovoltaic (TLPV) inverters may experience significant leakage currents due to the conductive channel and stray capacitance that develops between the ground and the PV array [9]–[11]. Depending on whether the solar cell is thin-film, polycrystalline, or monocrystalline, the value of this parasitic capacitance usually falls between 60 and 160 nF/kW [12]. In addition to endangering the safety of maintenance workers, leakage current can lead to increased harmonic distortion in the line current, interference of common-mode, and extra losses in the system. Therefore, international regulations establish rigorous restrictions on leakage current. For instance, the leakage current RMS value must stay below 300 mA in accordance with the VDE 0126-01-01 standard [13], [14].

Based on this background, numerous research efforts have focused on reducing leakage current and enhancing efficiency in TLPV inverters. In [15], a method was introduced where an additional power switch disconnects the PV array from the DC side to minimize leakage current. However, this switch causes significant power losses since it operates at a high frequency. In three-phase PV systems, the leakage current was effectively decreased by adding two additional switches to the traditional full-bridge (FB) inverter arrangement in [16] and [17]. In neutral-point clamped inverter and FB inverter topologies, an additional method described in [18] connects the grid's neutral point to the DC connection's midway. However, this arrangement needs more switches than the traditional FB inverter.

In study [7], a three-phase, full-bridge rectifier with zero-voltage topology was suggested, which uses twelve more diodes and two more switches than the typical FB inverter. Despite its effectiveness, this design greatly raises system costs and power losses. A fast recovery diode and a modulation approach intended to keep up a steady common-mode voltage (CMV) and one of a Z-source inverter's characteristics is its ability to lower leakage current shown in [19]. Similar to this, the reduced common-mode voltage PWM (RCMV-PWM) techniques suggested in [20] provide bipolar output voltage but have disadvantages including high switching losses, voltage spikes, and significant current ripples across filter inductors, which eventually reduce efficiency.

A new space-vector modulation (SVM) method for three-phase T-type inverters was proposed in [21] to further minimize leakage current. However, T-type inverters require more components than conventional inverter structures. Filter-clamped (FC) inverters are defined in this study as inverter setups that link the grid-side filter's neutral point to the DC link's midpoint. An inverter with three phases for a 50-kW transformerless system that reduces leakage current by connecting the neutral point of the filter to the DC-link's midway in [22] it was presented.

For variable-speed motor drives, another instance of attaching an LC filter to the DC-link midpoint has been investigated [23]. Nevertheless, findings from [23] are not directly suitable for TLPV systems employing LCL filters. In split DC link three-phase photovoltaic systems, neutral-point clamped and FB topologies were examined in [18] and [24], respectively, but these designs are not ideal for three-phase three-wire grids that lack a neutral conductor.

Additionally, split DC links and extra switches have been suggested for PV inverters that are single-phase in [25] and [26]. A half-bridge single-phase zero-voltage state rectifier was presented in [26]; in this, an active switch and diode rectifier connect the DC-link midway to the inverter's output. In a solar photovoltaic system connected to the grid with two stages and three phases without a transformer to effectively lower leakage current, a filter-clamped inverter topology was used in [27].

Application of the filter-clamped inverter in Figure 1, depicting TLPV grid-connected three-phase systems, is the main topic of this work. In this configuration, A DC/DC boost converter that connects the DC link to the PV array may be positioned, and to the DC link's midpoint, an LCL filter is linked [28]. This arrangement helps to significantly reduce leakage current, enhance the quality and efficiency of the current output, and minimize DC-link capacitor voltage ripples.

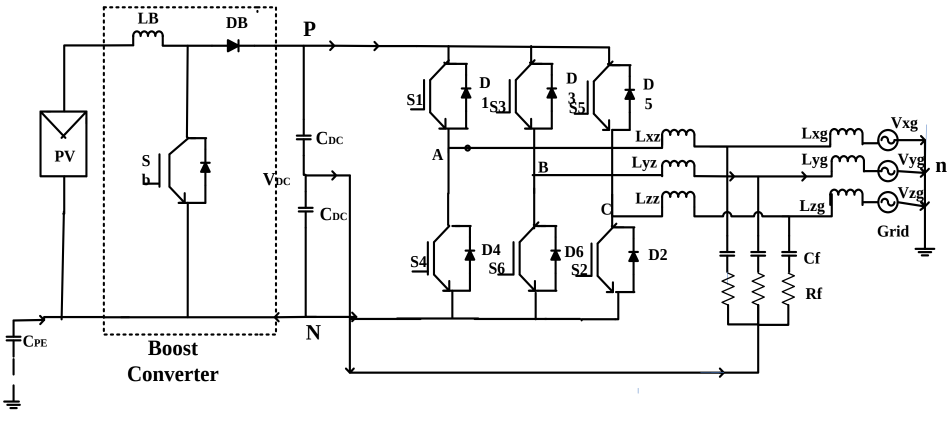

Figure 1. Filter-clamped grid-connected three-phase transformerless photovoltaic system

The proposed filter-clamped inverter (FCI) topology differs from previously reported inverter structures in several ways. Unlike the designs presented in [15]–[17], [19], and [21], as there are no extra components needed for the FCI. It produces a line-to-line voltage output that is unipolar, as opposed to [20], which reduces the line filter's voltage stress and power losses.

In contrast to the systems discussed in [22] and [27], a comprehensive mathematical model is presented in this paper, including the development of a common-mode equivalent circuit for detailed analysis. Moreover, the proposed FCI also operates reliably in three-phase, three-wire grid systems that lack a neutral conductor. This paper's primary contributions can be summed up as follows:

– The FCI is modified with a split DC link to successfully lower leakage current in three-wire, three-phase solar systems using an LCL output filter;
– To illustrate how the FCI reduces leakage current in PV applications, mathematical analysis and a common mode model are developed; and
– The FCI reduces leakage current without the need for additional parts like common-mode chokes or switches.

The structure of this paper is as follows: i) The mathematical analysis and leakage current modelling are represented in section 2 for three-phase TLPV systems using both FB and FC inverters, and discuss the control methodology of the proposed FCI system; ii) Section 3 includes the simulation results and discussions, respectively; iii) and Section 4 concludes the study with key findings on the performance and advantages of the FCI.

2. GRID-CONNECTED TRANSFORMERLESS PHOTOVOLTAIC SYSTEMS WITH LEAKAGE CURRENT: MATHEMATICAL ANALYSIS AND COMMON-MODE MODEL

2.1. Leakage current in full bridge inverter: mathematical analysis

A transformerless three-phase solar photovoltaic system with a FB inverter that is grid-connected is shown in Figure 2. In this configuration, a parasitic (stray) capacitance C_{PE} forms between the ground and PV module, allowing leakage current to pass through it. To suppress high-frequency harmonics generated by inverter switching, the utility grid and the inverter are connected via an LCL filter.

Figure 3 exhibits the FB inverter's common-mode circuit in a grid-connected configuration. In this circuit, the voltage across stray capacitance C_{PE} in this model is denoted as V_{PE}, and the resulting leakage current is expressed as I_{Leakage}. The voltages between the PV array's negative node N and the inverter output terminals (as shown in Figure 2) are represented by V_{xN}, V_{yN}, and V_{zN}. Similarly, the resistance between the ground and the grid neutral point n is represented by Rg, while V_{xg}, V_{yg}, and V_{zg} show the grid voltages for the three phases.

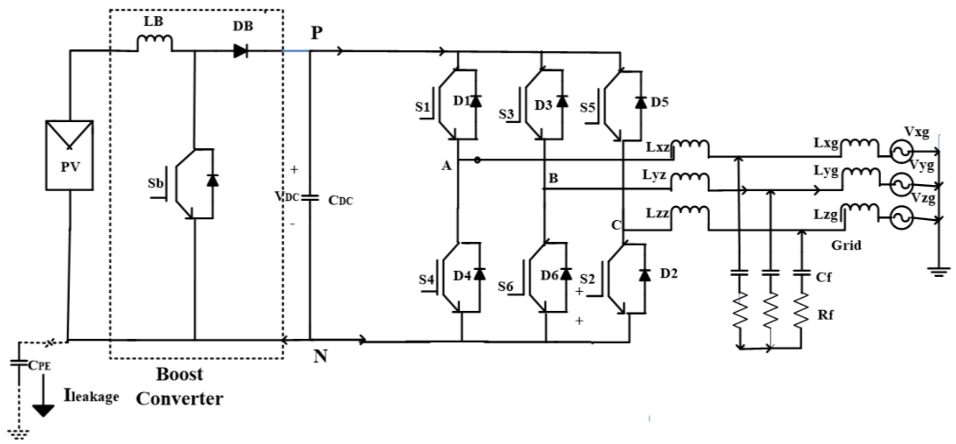

Figure 2. Three-phase transformerless photovoltaic (TLPV) full-bridge inverter for grid-connected systems

KCL and KVL are used on the equivalent common-mode circuit depicted in Figure 3 to determine the Leakage current of a grid-connected solar photovoltaic system that doesn't require a transformer. The voltage across CPE can be stated for each phase as follows, depending on the circuit configuration:

$$V_{PE} = -V_{xN} + sL_{x,z}I_{x,z} + sL_{x,g}I_{x,g} + V_{x,g} - R_g I_{\text{Leakage}} \quad (1)$$

$$V_{PE} = -V_{yN} + sL_{y,z}I_{y,z} + sL_{y,g}I_{y,g} + V_{y,g} - R_g I_{\text{Leakage}} \quad (2)$$

$$V_{PE} = -V_{zN} + sL_{z,z}I_{z,z} + sL_{z,g}I_{z,g} + V_{z,g} - R_g I_{\text{Leakage}} \quad (3)$$

The (1)-(3) describe the point-to-earth voltage V_{PE} for each phase (a, b, and c) of an inverter with three phases. They include the effects of phase-to-neutral voltage, coupling inductances, and phase-to-ground voltages. The inductive terms represent voltage variations caused by switching and parasitic elements. The ground resistance term accounts for the leakage current flowing to earth. Overall, the equations explain the origin of the system's leakage current and common-mode voltage.

The relationship between the current components in each phase is given by (4)-(6).

$$I_{x,z} = I_{x,f} + I_{x,g} \quad (4)$$

$$I_{y,z} = I_{y,f} + I_{y,g} \quad (5)$$

$$I_{z,z} = I_{z,f} + I_{z,g} \quad (6)$$

The (4)-(6) define the current relationship in each phase of the three-phase inverter system. For each phase, the total current $I_{(x,z)}$ is expressed as the sum of the filter current $I_{(x,f)}$ and the ground (leakage) current $I_{(x,g)}$. This shows how the phase current splits into different paths. The equations help in analyzing leakage current flow and current distribution in the inverter.

The summing of the ground currents yields the total leakage current passing through the parasitic path of all three phases is (7).

$$I_{\text{Leakage}} = -(I_{x,g} + I_{y,g} + I_{y,g}) \quad (7)$$

Since the inverter output currents satisfy the balanced condition by (8).

$$I_{x,f} + I_{y,f} + I_{z,f} = 0 \quad (8)$$

In the three-phase system, the expression for common-mode voltage is as in (9).

$$V_{CM} = \frac{V_{xN}+V_{yN}+V_{zN}}{3} \quad (9)$$

The (10) and (11) are true under balanced operating conditions.

$$V_{x,g} + V_{y,g} + V_{z,g} = 0 \quad (10)$$

$$L_{x,z} = L_{y,z} = L_{z,z} = L_z \text{and } L_{x,g} = L_{y,g} = L_{z,g} = L_g \quad (11)$$

Thus, the instantaneous leakage current via parasitic capacitance is described as (12),

$$I_{\text{Leakage}}(t) = C_{PE}\frac{dV_{PE}(t)}{dt} \quad (12)$$

or, equivalently, in the Laplace domain (13).

$$I_{\text{Leakage}} = sC_{PE}V_{PE} \quad (13)$$

The (12) demonstrates how the parasitic capacitance C_{PE} and the rate of change of the voltage across it, represented as $dV_{PE}(t)/dt$, affect the leakage current.

The (1)– (13) can be combined to express the parasitic capacitor's voltage V_{PE} as (14).

$$V_{PE} = \frac{3}{3+3sC_{PE}R_g+s^2C_{PE}(L_z+L_g)}\,(-V_{CM}) \quad (14)$$

The (14) indicates that the potential V_{PE} is directly linked to the CMV. Therefore, when the CMV fluctuates with time, there are notable voltage fluctuations across the parasitic capacitor C_{PE}, causing a large leakage current between the ground and the PV array. However, in the proposed FCI, the parasitic capacitor's voltage V_{PE} is independent of the CMV. This characteristic and its underlying conduct are thoroughly discussed in section 2.2.

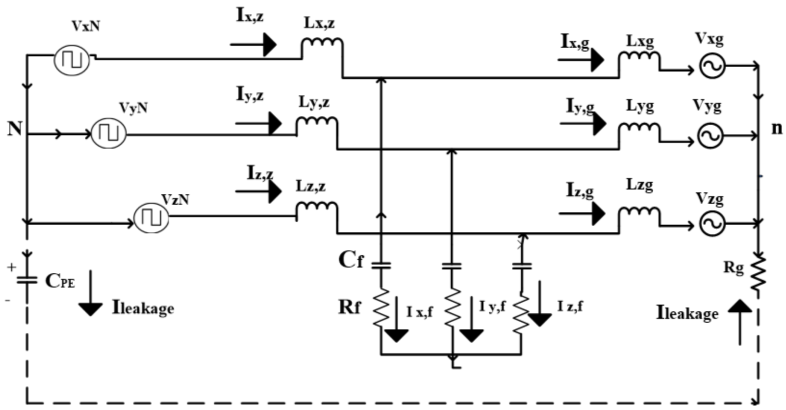

Figure 3. A three-phase transformerless photovoltaic full-bridge grid-connected inverter's common-mode model

2.2. Mathematical evaluation of leakage current in filter-clamped (FC) inverter

Figure 4 shows the schematic for the grid-connected filter-clamped inverter. The DC link's midway is attached to the LCL output filter's capacitor in this setup. The corresponding common-mode equivalent circuit is illustrated in Figure 5. Although the filter-clamped and full-bridge inverters employ the same control strategy, their layouts differ in the FCI; the neutral point is linked to the DC-link midway of the LCL filter, which alters the resulting common-mode behavior.

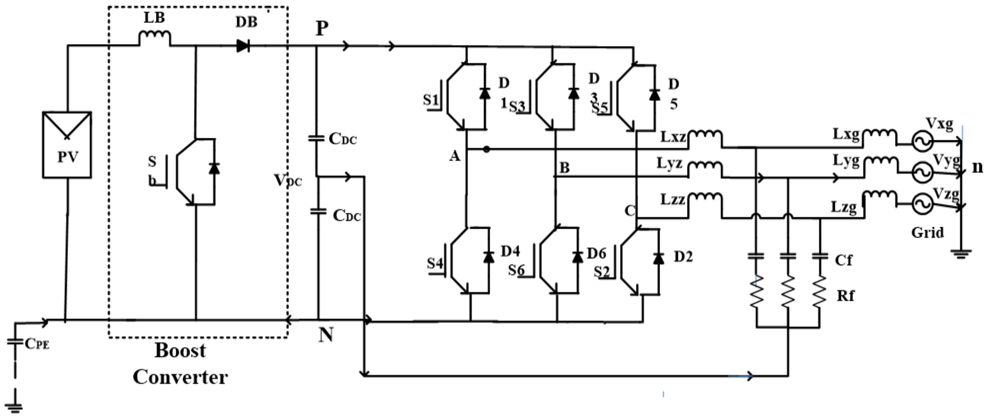

Figure 4. Three-phase grid-connected transformerless filter clamped inverter

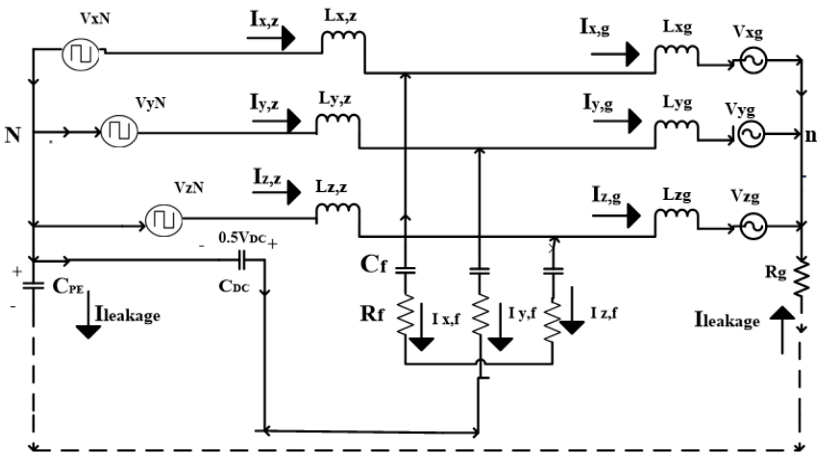

Figure 5. Three-phase TLPV grid-connected filter clamped inverters using a common mode model

The common-mode circuit in Figure 5 is subjected to KCL and KVL to investigate the FCI's leakage current. The (15)-(17) are the expressions for the resulting equations.

$$V_{PE} = -\frac{V_{DC}}{2} - V_{x,f} + sL_{x,g}I_{x,g} + V_{x,g} - R_g I_{\text{Leakage}} \quad (15)$$

$$V_{PE} = -\frac{V_{DC}}{2} - V_{y,f} + sL_{y,g}I_{y,g} + V_{y,g} - R_g I_{\text{Leakage}} \quad (16)$$

$$V_{PE} = -\frac{V_{DC}}{2} - V_{z,f} + sL_{z,g}I_{z,g} + V_{z,g} - R_g I_{\text{Leakage}} \quad (17)$$

The (15)-(17) describe the point-to-earth voltage V_{PE} for the inverter's phases a, b, and c while taking the DC-link voltage into account. The term $-\frac{V_{DC}}{2}$ represents the contribution of the DC bus's midway voltage, while $V_{(x,f)}$denotes the filter voltage of each phase. The inductive terms account for grounding inductance effects during switching. The phase-to-ground voltage and ground resistance terms represent the impact of leakage current flow.

In this instance, the voltages across the LCL filter's RC branches are represented as $V_{x,f}$, $V_{y,f}$, and $V_{z,f}$. The (10)-(12) and (15)-(17) are combined. One way to describe the voltage across the parasitic capacitance V_{PE} is as (18).

$$V_{PE} = -\frac{\frac{3}{2}V_{DC}+(V_{x,f}+V_{y,f}+V_{z,f})}{3+3sC_{PE}R_g+s^2C_{PE}L_g} \quad (18)$$

The (18) makes it clear that the voltages across the LCL filter's RC branches and the voltage of the DC-link have the most effect on the potential VPE. In contrast to a conventional full-bridge inverter, where V_{PE} depends on the CMV (as indicated in (14)), the FCI topology ensures that $V_{PE}$is independent of CMV. As a result, no transient voltage is generated across the parasitic capacitance C_{PE} as a result of changes in CM, effectively reducing leakage current.

Impulse-like currents are suppressed in the FCI topology by connecting the RC branches to the grid from the LCL filter and the inverter via inductors. As a result, the voltages across the RC branches don't change effectively, eliminating abrupt transitions. The total voltage of the three RC branches $\left(V_{x,f} + V_{y,f} + V_{z,f}\right)$ forms a smooth waveform with a zero average value. Consequently, the voltage V_{PE} in the proposed FCI maintains a steady DC bias with minimal ripple, resulting in a significant reduction of leakage currents opposed to the traditional full bridge inverter. This observation was further verified through detailed simulation presented in the subsequent sections.

Figure 6 shows the system's configuration and its closed-loop control scheme. A P&O MPPT algorithm is used to track the PV array operating point, which provides the DC-link referencevoltage V_{dc}^*. A PI controller then processes this voltage to produce the active-power reference P*.

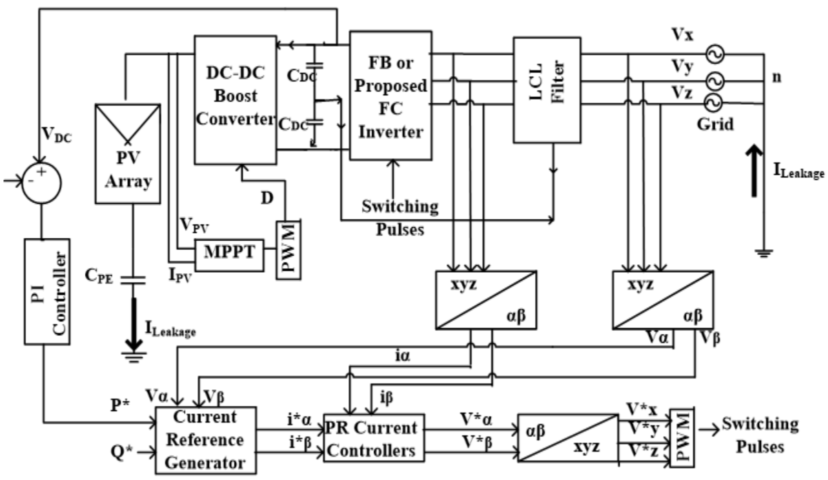

Figure 6. Block diagram of grid-connected three-phase transformerless photovoltaic system with a filter-clamped inverter

The inverter, operating in either FB or FC configuration, injects active power into the grid. The following equations demonstrate how the grid-synchronization currents are computed in αβ's stationary reference frame from the reactive and active power commands.

$$i_\alpha^* = \frac{1}{(V_\alpha^2 + V_\beta^2)} (V_\alpha P^* + V_\beta Q^*) \quad (17)$$

$$i_\beta^* = \frac{1}{(V_\alpha^2 + V_\beta^2)} (V_\beta P^* - V_\alpha Q^*) \quad (18)$$

At the LCL filter's grid side, V_g is monitored, and at inverter terminals, the phase currents are sensed (Figure 6). This sensing arrangement improves control accuracy by providing precise voltage and current feedback.

3. SIMULATION RESULTS AND DISCUSSIONS

To evaluate the FCI performance, a comprehensive simulation model was created in MATLAB/Simulink, particularly its effectiveness in suppressing leakage current. Both inverter topologies—the FB and the FC, shown earlier in Figures 2 and 4 were modeled within the same framework for comparative evaluation. Figures 7 and 8 depict the grid currents in three phases for the full bridge and the filter-clamped inverter, respectively. Figures 7 and 8 show the simulated grid currents in three phases of a B6 inverter and a B6 clamped inverter plotted against time. All three phase currents are sinusoidal and balanced, with equal magnitude. Each waveform is phase-shifted by 120°, which is characteristic of a three-phase system. Small ripples appear because of the inverter's switching action.

Figures 9 and 10 illustrate the voltage across the stray capacitance (V_{PE}) for both inverter types. The FB inverter exhibits considerable fluctuations in V_{PE}, while the FCI maintains a nearly constant and stable V_{PE}. Figure 9 shows the simulated stray capacitor voltage of a B6-type inverter plotted versus time. The voltage waveform exhibits high-frequency oscillations caused by inverter switching. Large voltage fluctuations indicate the effect of parasitic capacitances and common-mode voltage. Figure 10 illustrates the simulated stray capacitance voltage of a B6 clamped inverter with respect to time. The waveform shows high-frequency oscillations due to inverter switching and parasitic capacitances. Compared to a conventional B6 inverter, the voltage fluctuations are reduced, indicating better clamping action.

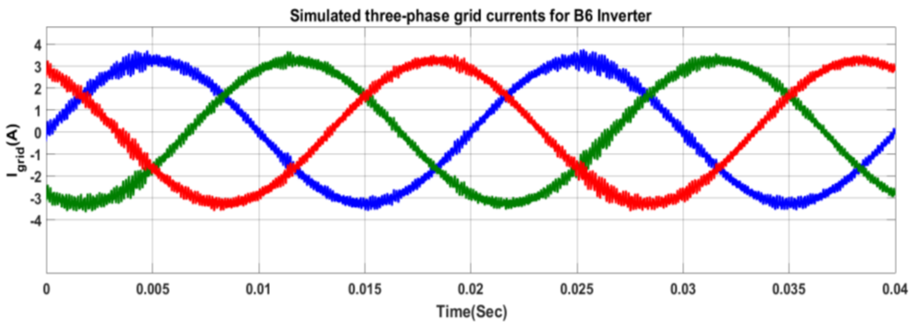

Figure 7. Grid currents injected by the transformerless photovoltaic FB inverter

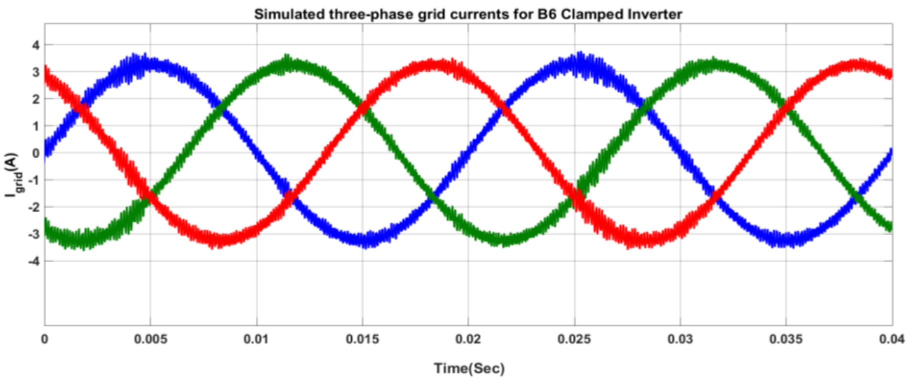

Figure 8. Grid currents injected by the TLPV FC inverter

Consequently, as shown in Figure 11, the FB inverter experiences large leakage current, with an RMS value of approximately 600 mA, exceeding the 300 mA safety threshold defined in international standards as shown in Table 1. In contrast, the FCI's leakage current waveform, which keeps an RMS value of about 70 mA, is shown in Figure 12, well below the allowable limit specified by grid safety standards. Thus, the filter-clamped inverter effectively mitigates leakage current and satisfies the VDE 0126-1-1 safety requirements. These simulation outcomes confirm the validity of the analytical models developed and discussed in section 2, demonstrating that the FCI achieves lower leakage current when compared to the FB inverter. Figures 13 and 14 are the waveforms of three-phase grid voltages for FB and FC inverters. Figures 13 and 14 represent the simulated three-phase grid voltages of a B6 inverter and a B6 Clamped inverter. All three-phase voltages are balanced, sinusoidal, and 120° phase-shifted from each other. The amplitudes remain nearly equal, indicating proper voltage control and symmetry. Small ripples on the waveforms are due to PWM switching effects of the inverter.

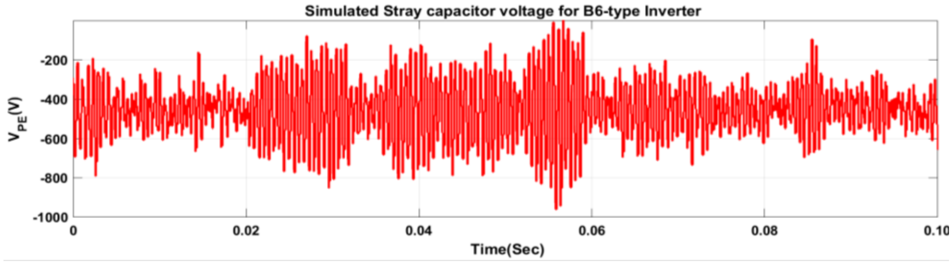

Figure 9. Stray capacitance voltage (V_{PE}) for TLPV FB inverter

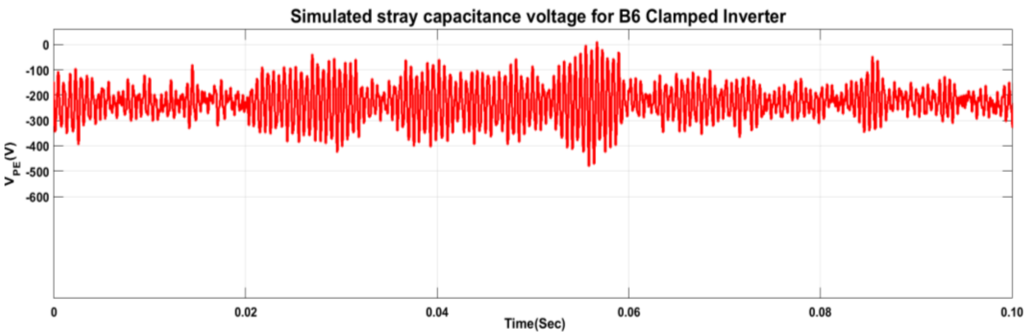

Figure 10. Stray capacitance voltage (V_{PE}) for TLPV FC inverter

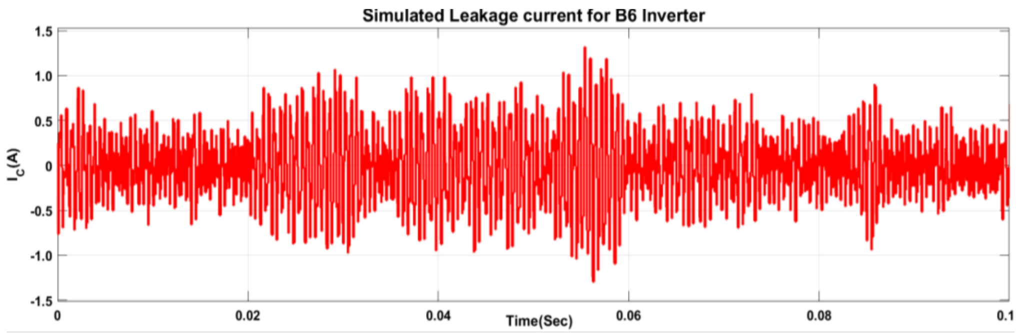

Figure 11. Leakage current for transformerless photovoltaic FB inverter connected to grid

Table 1. Leakage current in FB and proposed FC type inverters

Type of inverter	FB inverter	FC inverter
Leakage current	600 mA	70 mA

The parameters used for all the simulation in this paper are: At LCL filter: The LCL filter's damping resistor Rf = 5.6 Ω, the LCL filter's inverter side inductor Lc = 6.5 mH, The LCL filter's capacitor Cf = 2.2 µF. At grid side filter: The LCL filter's grid side inductor, Lg = 0.65 mH, 50 Hz is the grid frequency, nominal voltage from one phase to another (Vrms) = 220 V; two capacitors connected in series form a DC link capacitor. (CDC) = 680 µF, Resistor between the grid ground and the array's stray capacitance, Rg = 11 Ω and switching frequency = 16 kHz. As per Table 1, in FCI, the leakage current is significantly reduced in comparison to the FB inverter that is from 600 mA to 70 mA.

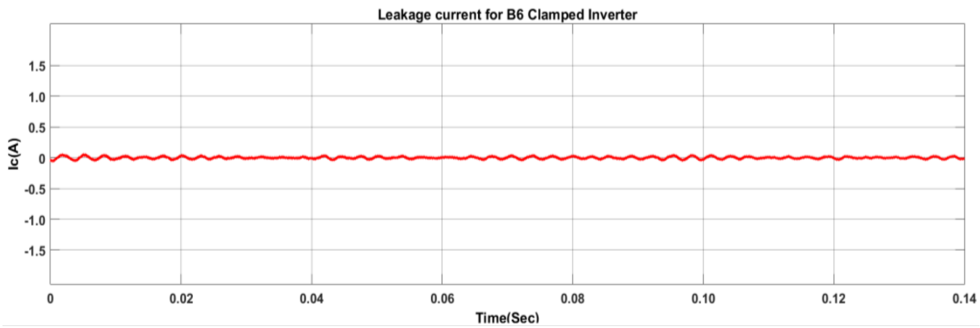

Figure 12. Leakage current of grid-connected transformerless photovoltaic FC inverter

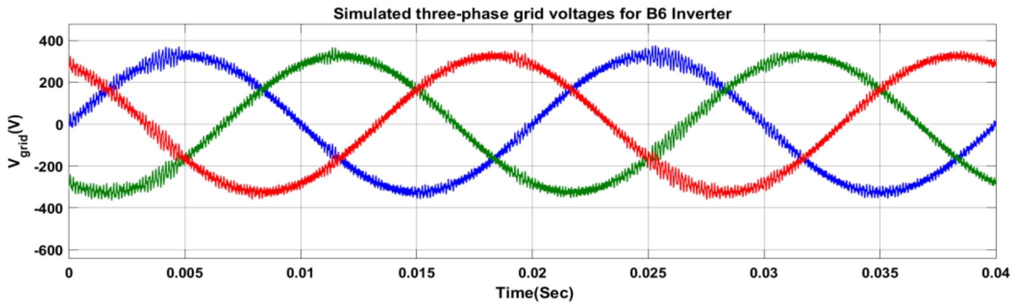

Figure 13. Three-phase grid voltages for FB inverter

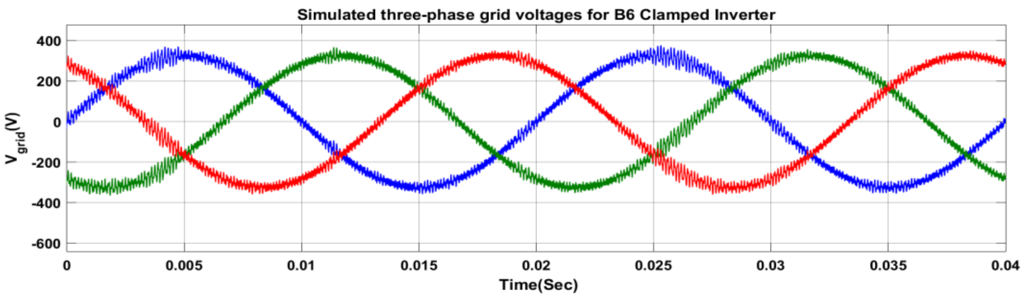

Figure 14. Three-phase grid voltages for FC inverter

4. CONCLUSION

This study proposes the FC inverter for reducing three-phase photovoltaic systems leakage current without transformers. The PV stray-capacitance voltage is separated from the common-mode voltage by connecting the output filter to the DC-link's midpoint, thereby lowering leakage current. To examine leakage current behavior of each, a common-mode comparable model was created for the proposed FC inverter and the conventional full-bridge inverter. Results of the simulation showed that the FCI significantly outperformed the FB inverter, reducing leakage current from 600 mA to 70 mA. Leakage current was significantly suppressed by the FCI. Consequently, the suggested filter-clamped inverter topology offers a reliable and cost-effective alternative for future grid-connected TLPV systems.

FUNDING INFORMATION

According to the authors, there is no funding involved.

AUTHOR CONTRIBUTIONS STATEMENT

This journal uses the Contributor Roles Taxonomy (CRediT) to recognize individual author contributions, reduce authorship disputes, and facilitate collaboration.

Name of Author	C	M	So	Va	Fo	I	R	D	O	E	Vi	Su	P	Fu
Mohammed Abdullah	✓	✓	✓	✓	✓	✓	✓	✓	✓	✓			✓	
S. Venkata Padmavathi	✓									✓		✓		

C : **C**onceptualization
M : **M**ethodology
So : **So**ftware
Va : **Va**lidation
Fo : **Fo**rmal analysis
I : **I**nvestigation
R : **R**esources
D : **D**ata Curation
O : Writing - **O**riginal Draft
E : Writing - Review & **E**diting
Vi : **Vi**sualization
Su : **Su**pervision
P : **P**roject administration
Fu : **Fu**nding acquisition

CONFLICT OF INTEREST STATEMENT

Authors state no conflict of interest.

DATA AVAILABILITY

Data availability is not applicable to this paper as no new data were created or analyzed in this study.

REFERENCES

[1] C. Zhang, S. Du, and Q. Chen, "A novel scheme suitable for high-voltage and large-capacity photovoltaic power stations," *IEEE Transactions on Industrial Electronics*, vol. 60, no. 9, pp. 3775–3783, Sep. 2013, doi: 10.1109/TIE.2012.2208438.

[2] E. Bullich-Massagué, R. Ferrer-San-José, M. Aragüés-Peñalba, L. Serrano-Salamanca, C. Pacheco-Navas, and O. Gomis-Bellmunt, "Power plant control in large-scale photovoltaic plants: design, implementation and validation in a 9.4 MW photovoltaic plant," *IET Renewable Power Generation*, vol. 10, no. 1, pp. 50–62, Jan. 2016, doi: 10.1049/iet-rpg.2015.0113.

[3] M. Farhadi and M. Abapour, "Three-switch three-phase inverter with improved DC voltage utilization," *IEEE Transactions on Industrial Electronics*, vol. 66, no. 1, pp. 14–24, Jan. 2019, doi: 10.1109/TIE.2018.2829680.

[4] S. Farzam Kia, H. Iman-Eini, and S. Farhangi, "Increasing the number of voltage levels in single-phase multilevel converters," *6th Annual International Power Electronics, Drive Systems, and Technologies Conference, PEDSTC 2015*, pp. 591–596, 2015, doi: 10.1109/PEDSTC.2015.7093341.

[5] M. Farhadi, M. Abapour, and M. Sabahi, "Failure analysis and reliability evaluation of modulation techniques for neutral point clamped inverters—A usage model approach," *Engineering Failure Analysis*, vol. 71, pp. 90–104, Jan. 2017, doi: 10.1016/j.engfailanal.2016.06.010.

[6] M. Farhadi, M. Abapour, and B. Mohammadi-Ivatloo, "Reliability analysis of component-level redundant topologies for solid-state fault current limiter," *International Journal of Electronics*, vol. 105, no. 4, pp. 541–558, Apr. 2018, doi: 10.1080/00207217.2017.1378380.

[7] M. Imran and M. Mane, "Comparative study on analysis of losses and leakage current for transformer-less inverters for PV applications: a review," *International Journal for Research in Applied Science and Engineering Technology*, vol. 11, no. 9, pp. 152–158, Sep. 2023, doi: 10.22214/ijraset.2023.55624.

[8] M. Imran, "Enhanced performance of single-phase transformer-less inverter for grid-connected photovoltaic systems with leakage current reduction," *Journal of Information Systems Engineering and Management*, vol. 10, no. 39s, pp. 599–608, 2025, doi: 10.52783/jisem.v10i39s.7247.

[9] A. K. Gupta, H. Agrawal, and V. Agarwal, "A novel three-phase transformerless H-8 topology with reduced leakage current for grid-tied solar PV applications," *IEEE Transactions on Industry Applications*, vol. 55, no. 2, pp. 1765–1774, Mar. 2019, doi: 10.1109/TIA.2018.2883372.

[10] V. Sonti and S. Jain, "DC decoupling-based three-phase three-level transformerless PV inverter topology for minimization of leakage current," *IEEE Transactions on Industrial Electronics*, vol. 66, no. 10, pp. 8273–8278, Oct. 2019, doi: 10.1109/TIE.2018.2869364.

[11] X. Guo, N. Wang, B. Wang, Z. Lu, and F. Blaabjerg, "Evaluation of three-phase transformerless DC-bypass PV inverters for leakage current reduction," *IEEE Transactions on Power Electronics*, vol. 35, no. 6, pp. 5918–5927, Jun. 2020, doi: 10.1109/TPEL.2019.2954298.

[12] G. I. Orfanoudakis, E. Koutroulis, G. Foteinopoulos, and W. Wu, "Analysis and reduction of common-mode ground leakage current in transformerless PV inverters with rectified sine wave DC-link voltage," *Journal of Power Electronics*, vol. 26, no. 1, pp. 227–241, Jan. 2026, doi: 10.1007/s43236-025-01106-1.

[13] R. Rahimi, E. Afshari, B. Farhangi, and S. Farhangi, "Optimal placement of additional switch in the photovoltaic single-phase grid-connected transformerless full bridge inverter for reducing common mode leakage current," in *2015 IEEE Conference on Energy Conversion (CENCON)*, Oct. 2015, pp. 408–412, doi: 10.1109/CENCON.2015.7409579.

[14] M. C. Cavalcanti, A. M. Farias, K. C. Oliveira, F. A. S. Neves, and J. L. Afonso, “Eliminating leakage currents in neutral point clamped inverters for photovoltaic systems,” *IEEE Transactions on Industrial Electronics*, vol. 59, no. 1, pp. 435–443, Jan. 2012, doi: 10.1109/TIE.2011.2138671.
[15] T. K. S. Freddy, N. A. Rahim, W.-P. Hew, and H. S. Che, “Modulation techniques to reduce leakage current in three-phase transformerless H7 photovoltaic inverter,” *IEEE Transactions on Industrial Electronics*, vol. 62, no. 1, pp. 322–331, Jan. 2015, doi: 10.1109/TIE.2014.2327585.
[16] R. Rahimi, S. Farhangi, B. Farhangi, G. R. Moradi, E. Afshari, and F. Blaabjerg, “H8 inverter to reduce leakage current in transformerless three-phase grid-connected photovoltaic systems,” *IEEE Journal of Emerging and Selected Topics in Power Electronics*, vol. 6, no. 2, pp. 910–918, Jun. 2018, doi: 10.1109/JESTPE.2017.2743527.
[17] R. Rahimi, B. Farhangi, and S. Farhangi, “New topology to reduce leakage current in three-phase transformerless grid-connected photovoltaic inverters,” in *2016 7th Power Electronics and Drive Systems Technologies Conference (PEDSTC)*, Feb. 2016, pp. 421–426, doi: 10.1109/PEDSTC.2016.7556898.
[18] T. Kerekes, R. Teodorescu, M. Liserre, C. Klumpner, and M. Sumner, “Evaluation of three-phase transformerless photovoltaic inverter topologies,” *IEEE Transactions on Power Electronics*, vol. 24, no. 9, pp. 2202–2211, Sep. 2009, doi: 10.1109/TPEL.2009.2020800.
[19] F. Bradaschia, M. C. Cavalcanti, P. E. P. Ferraz, F. A. S. Neves, E. C. dos Santos, and J. H. G. M. da Silva, “Modulation for three-phase transformerless Z-Source inverter to reduce leakage currents in photovoltaic systems,” *IEEE Transactions on Industrial Electronics*, vol. 58, no. 12, pp. 5385–5395, Dec. 2011, doi: 10.1109/TIE.2011.2116762.
[20] A. M. Hava and E. Un, “Performance analysis of reduced common-mode voltage PWM methods and comparison with standard PWM methods for three-phase voltage-source inverters,” *IEEE Transactions on Power Electronics*, vol. 24, no. 1, pp. 241–252, Jan. 2009, doi: 10.1109/TPEL.2008.2005719.
[21] T. Yu, W. Wan, and S. Duan, “A modulation method to eliminate leakage current and balance neutral-point voltage for three-level inverters in photovoltaic systems,” *IEEE Transactions on Industrial Electronics*, vol. 70, no. 2, pp. 1635–1645, Feb. 2023, doi: 10.1109/TIE.2022.3161809.
[22] T. Zhao, V. Bhavaraju, P. Nirantare, and J. Xu, “Evaluation of commercial scale transformerless solar inverter technology,” in *2015 IEEE Energy Conversion Congress and Exposition (ECCE)*, Sep. 2015, pp. 5342–5348, doi: 10.1109/ECCE.2015.7310411.
[23] M. Farhadi, M. T. Fard, M. Abapour, and M. T. Hagh, “DC-ac converter-fed induction motor drive with fault-tolerant capability under open- and short-circuit switch failures,” *IEEE Transactions on Power Electronics*, vol. 33, no. 2, pp. 1609–1621, 2018, doi: 10.1109/TPEL.2017.2683534.
[24] T. Kerekes, R. Teodorescu, and U. Borup, “Transformerless photovoltaic inverters connected to the grid,” in *APEC 07 - Twenty-Second Annual IEEE Applied Power Electronics Conference and Exposition*, Feb. 2007, pp. 1733–1737, doi: 10.1109/APEX.2007.357753.
[25] T. Kerekes, R. Teodorescu, P. Rodriguez, G. Vazquez, and E. Aldabas, “A new high-efficiency single-phase transformerless PV inverter topology,” *IEEE Transactions on Industrial Electronics*, vol. 58, no. 1, pp. 184–191, Jan. 2011, doi: 10.1109/TIE.2009.2024092.
[26] L. Zhang, K. Sun, L. Feng, H. Wu, and Y. Xing, “A family of neutral point clamped full-bridge topologies for transformerless photovoltaic grid-tied inverters,” *IEEE Transactions on Power Electronics*, vol. 28, no. 2, pp. 730–739, 2013, doi: 10.1109/TPEL.2012.2205406.
[27] R. Rahimi, M. Farhadi, G. R. Moradi, B. Farhangi, and S. Farhangi, “Filter-clamped two-level three-phase transformerless grid-connected photovoltaic inverter for leakage current reduction,” *SSRN Electronic Journal*, 2020, doi: 10.2139/ssrn.3567399.
[28] F. Elghabsi *et al.*, “High gain and high efficiency soft switching quadratic boost converter for renewable energy applications,” *Scientific Reports*, vol. 15, no. 1, 2025, doi: 10.1038/s41598-025-20207-2.

BIOGRAPHIES OF AUTHORS

Mohammed Abdullah received his bachelor's degree in electrical and electronics engineering in 2002 and his master's degree in energy systems in 2008 from Jawaharlal Nehru Technological University, Hyderabad, India. He is currently pursuing his Ph.D. degree in electrical,electronics and communication engineering at GSCE, GITAM Deemed to be University, Hyderabad Campus, India. Since 2010, he has been working as an assistant professor in the Department of Electrical Engineering at Muffakham Jah College of Engineering and Technology, Hyderabad, India. His research interests include renewable energy, power electronics, motor drives, and the application of power electronics in renewable energy systems. He can be contacted at email: abdullaheed@mjcollege.ac.in.

S. Venkata Padmavathi received her bachelor's degree in electrical and electronics engineering from GMR Institute of Technology, Rajam, India, in 2003 and her master's degree in power systems engineering from Thiagarajar College of Engineering, Madurai, India, in 2006. She received her Ph.D. degree in electrical engineering from Jawaharlal Nehru Technological University Hyderabad, Hyderabad, India. She is currently working as an assistant professor at GSCE, GITAM Deemed to be University, Hyderabad Campus, India. She has authored more than 30 scholarly articles in the areas of power system security, power quality, and flexible alternating current transmission systems, published in reputable international journals and conference proceedings. She can be contacted at email: vsatyava@gitam.edu.